Adsorption of Amino Acids on Gold: Assessing the Accuracy of the GolP-CHARMM Forcefield and Parametrization of Au-S Bonds

Zdenek Futera[1] *and Jochen Blumberger*[1,2*]

[1]University College London, Department of Physics and Astronomy and Thomas-Young-Centre, Gower Street, London WC1E 6BT, UK

[2]Institute for Advanced Study, Technische Universität München, Lichtenbergstrasse 2 a, D-85748 Garching, Germany

Abstract

The interaction of amino acids with metal electrodes plays a crucial role in bioelectrochemistry and the emerging field of bionanoelectronics. Here we present benchmark calculations of the adsorption structure and energy of all natural amino acids on Au(111) in vacuum using a van-der-Waals density functional (revPBE-vdW) that showed good performance on the S22 set of weakly bound dimers (mean relative unsigned error (MRUE) wrt CCSD(T)/CBS = 13.3%) and adsorption energies of small organic molecules on Au(111) (MRUE wrt experiment = 11.2%). The vdW-DF results are then used to assess the accuracy of a popular force field for Au-amino acid interactions, GolP-CHARMM, which explicitly describes image charge interactions via rigid-rod dipoles. We

* Corresponding authors: j.blumberger@ucl.ac.uk, z.futera@ucl.ac.uk; Tel: ++44-(0)20-7679-4373 (JB), Fax: ++44-(0)20-7679-7145 (both)

find that whilst the force field underestimates adsorption distances, it does reproduce the binding energy rather well (MRUE wrt to revPBE-vdW = 11.3%) with the MRUE decreasing in the order Cys, Met > amines > aliphatic > carboxylic > aromatic. We also present a parameterization of the bonding interaction between sulfur- containing molecules and the Au(111) surface and report force field parameters that are compatible with GolP-CHARMM. We believe the vdW-DF calculations presented herein will provide useful reference data for further force field development, and that the new Au-S bonding parameters will enable improved simulations of proteins immobilized on Au-electrodes via S-linkages.

I. Introduction

Molecular bioelectronics has been a rapidly growing field during the last decade utilizing unique electronic properties of metal / organic interfaces and finding various applications in electronics, photonics, biosensing or catalysis [1, 2]. Electron transport through self-assembled monolayers as well as electronic conductance of molecular arrays and single (macro)molecules have been investigated in bioelectronic devices [3, 4, 5]. Several advanced methods allowing fabrication and measurements of the metal contacts with biomacromolecules were developed such as electron beam lithography (EBL) [6, 7], scanning tunnelling microscopy (STM) [8], conductive probe atomic force microscopy (CP-AFM) [9] or the suspended nanowire junction technique [10, 11, 12]. Special interest has focused on electron transport properties of metalloprotein containing cofactors with incorporated transition-metal cations, which often participate in the electron transport via their molecular redox states [13, 14, 15, 16, 17, 18, 19, 20, 21, 22].

For accurate charge-transport measurements on the proteins their immobilization on the substrate surface is often desired [23]. Although proteins adsorb passively (i.e. physisorb) on the gold surfaces, covalent anchoring is usually needed to attach proteins to the surface at specific sites to avoid drift and diffusion along and away from the surface. Self-assembled monolayers of organic chains covalently bound to the surface by sulfur-based head groups is often utilized on gold surfaces as interfacial layer to which the protein is chemically bound. However, direct attachment of the protein to the surface (i.e. chemisorption), typically via cysteine sulfur, is the preferred approach with less uncertainties in geometry. Moreover, charge transport on metal / protein interfaces is measured directly on chemisorbed structures without need to tunnel through the mediating self-assembled monolayers. Many pioneering studies were performed on the blue copper protein Azurin [16, 24, 25, 26, 27] or heme-containing cytochrome c [28, 29, 30, 31, 32] because of their small size, stable structure, presence of anchoring cysteines and efficient intra-molecular charge transport across these proteins. In addition, conductivity measurements in a single-molecular junction setup were successfully carried out on more complex proteins such as photosystem I [33].

Electronic properties of proteins are usually measured on noble-metal electrodes which have clean surfaces and are mostly chemically inert under ambient conditions in addition to being excellent conductors. There has been a lot of effort in the past decade to describe protein interactions with metals, especially gold, by empirical force-field potentials that would allow one to carry out large-scale molecular dynamics (MD) simulations of protein/Au interfaces. In most cases well-tested biomolecular force fields such as Amber [34, 35], CHARMM [36, 37, 38, 39, 40] or CVFF [37, 41] were applied where the interaction with the metal was added in form of suitably fitted Lennard-Jones (LJ) potentials [42, 43]. An obvious advantage of this approach is its

simplicity and straightforward implementation in standard software packages. However, these simple models entirely disregard image charge interactions, which is typical for highly polarizable metallic surfaces like gold. Although some researchers discussed that this interaction is very weak and practically negligible because of its short-range character and dominant LJ interaction near the surface [35, 36], Heinz et al. estimated the strength of the image charge interaction a posteriori on structure samples from MD on Au(111) concluding that the average polarization energy of water in the first hydration layer is not insignificant, -2.38 kJ/mol, and it drops to -0.13 kJ/mol in the second layer [44].

Polarization effects on metallic interfaces were first introduced in molecular mechanics in the so-called discrete classical model (DCM) of Finnis *et al.* [45, 46, 47], which involves a set of induced point charges and dipoles assigned to each metal atom, responding to the external electrostatic field due to the adsorbent. Siepmann and Sprik described the charge density in metals by Gaussian distributions located on metallic sites and dynamically responding to external fields in an extended Lagrangian formalism [48]. Later, Iori *et al*. [49, 50] constructed the GolP force field specific for the Au(111) surface where the gold slab is made polarizable via an ensemble of rigid-rod dipoles attached to the gold atoms. Such description is conceptually similar to the Drude shell model where fictitious charged particles oscillate in a harmonic potential centred on the metal and responding to an external field [51]. Substitution of the Drude particles by rigid-rod dipoles in GolP allows one to retain long MD time steps common in biomolecular simulations (1-2 fs) while keeping the dynamics numerically stable. Recently, Wright *et al*. [52] reparametrized the original GolP, that is based on the OPLS-AA force field [53, 54], for use in combination with the CHARMM force field. In addition to Au (111), also the Au (100) surface is available in GolP-CHARMM. The image charge interaction was recently also introduced in a QM/MM formalism,

where the classically described metal is self-consistently polarized by charge density of an adsorbent treated at a quantum level of theory [55].

The basis for a successful description of protein-gold interactions is an accurate treatment of the interactions at a single amino acid level. Feng *et al*. [37] examined adsorption of all twenty one amino acids on Au(111) in aqueous solution showing that the adsorption energy is determined by molecular size and geometry rather than by specific chemistry. Large amino acids such as Arg, Trp, Gln, Tyr and Asn were found as the strongest adsorbents. Later, Hoefling *et al*. [56] evaluated adsorption free energy of amino acids in water capped by acetyl groups using the polarizable GolP force field [49, 50] concluding that there is a general trend with the type of amino acid: aromatic < sulfur < positive < polar < aliphatic ~ negative. Due to the conformational effects lowering the surface interaction, the adsorption energy of a peptide chain is lower than the sum of the adsorption energies of the involved amino acids [39, 57]. Binding energies of all amino acids in solution on Au(111) surface were evaluated by Nawrocki and Cieplak in different force fields concluding that they are not additive in protein structures [58]. Besides the force-field studies, density functional theory (DFT) was also employed to evaluate adsorption energies of individual amino acids on the Au(111) surface in vacuum at a quantum level of theory. However, these studies suffered from a lack of dispersion interaction, which is of course of great importance at polarizable metallic interfaces [59, 60, 61].

Adsorption of small proteins on a gold surfaces have been studied as well. Yu et al. [62] investigated protein physisorption in solution, which is relevant for bioelectrochemical experiments, and identified four stages of the adsorbing process: diffusion, anchoring, crawling and binding. The heme-containing electron-transfer protein cytochrome c was simulated at a solution interface with a gold surface using GolP and GolP-CHARMM force fields [63, 64].

Although the covalent interaction between gold and the anchoring cysteine was not included in the model and the cytochrome was allowed to drift on the surface, the adsorption structure obtained and the electron transfer rate predicted were in remarkable agreement with experimental data [65]. Chemisorption was modelled in simulations of plastocyanine on non-polarizable Au(111) surface, where one or both sulfur atoms from a dissociated disulfide bridge was covalently bound to the gold surface [40].

While the GolP force field has been a major step forward, its accuracy towards the description of amino acid-gold adsorption structures and energies is not well established. This is due to a lack of suitable reference data that would allow one to benchmark the force field. In an effort to fill this gap, we present here accurate DFT refence data for adsorption of small molecules for which experimental data are available, and of all twenty natural amino acids on the Au(111) surface in vacuum. Of all functionals investigated, we find that revPBE-vdW (known in literature also as vdW-DF) [66, 67, 68, 69] gives best performance for small molecules when compared to experimental reference data. The mean relative unsigned errors (MRUEs) of adsorption energies and distances in GolP-CHARMM are 11.2 % and 5.3 %, respectively, compared to revPBE-vdW on the set of small molecules. The force field performs similarly well for the amino acids with corresponding errors of 11.3 % and 7.8 %. In particular, the normalized, size-independent adsorption energies of the amino-acid types as predicted by revPBE-vdW is well reproduced by GolP-CHARMM: Cys, Met > aliphatic > amines > aromatic > amides > hydroxylic > carboxylic.

A second aim of this work is to provide accurate parameters for Au-S covalent bonding that can be used in combination with the GolP-CHARMM force field. These parameters are currently missing, although they are essential because in many applications proteins chemisorb on gold via natural or engineered cysteines. Here we report parameters obtained from calculations of

potential energy profiles between Au(111) and sulfur in several small molecules including cysteine. The new parameters for Au-S covalent bonding together with the assessment of the GolP-CHARMM force field opens up more realistic calculations of protein/Au interfaces and informs on the expected accuracy of molecular simulations in the emerging field of nanobioelectronics.

The article is structured as follows. First, we validate our DFT setup, which we will use as a reference for the adsorption structure and energetics of individual amino acids. In the second part of the manuscript, we present benchmark calculations of various small molecules and set of neutral amino acids on vacuum Au(111) surface as evaluated in GolP-CHARMM force field. Then, we discuss covalent interaction of three sulfur-containing small molecules with gold surface and its parameterization in the force field. Finally, we summarize the main results in the last part of the paper.

II. Computational Details

For validation of the GolP-CHARMM force field set-up and reference DFT calculations, we first calculated adsorption energies of small molecules which were originally used to fit and test the force field [52]. The former, hereafter referred to as ``fitting set" consists of methane (CH4), ethane (ETH), butane (BUT), hexane (HEX), heptane (HEP), octane (OCT), nonane (NON), ethene (ETE), 1,3-butadiene (BDE), benzene (BEN), methanethiol (MTH), diethylsulfide (DES), methylamine (MAM), imidazole (IMI), and water (WTR). The latter, hereafter referred to as ``test set" consists of cyclohexane (CHX), *trans*-2-butene (TBU), non-1-en (NEN), cyclohexene (CHE), toluene (TOL), methanol (MOH), acetone (ACT), formic acid (FMA), ammonia (AMM),

formamide (FMN), ethanethiol (ESH), and dibutylsulfide (DBS). Then calculations were carried out on all natural amino acids except selenocysteine (twenty amino acids in total) in their neutral protonation state.

The molecules were adsorbed on the closed-packed Au(111) surface, which was modelled by a four-layer $4\sqrt{3} \times 7$ slab consisting of 224 gold atoms. The lattice constant was set to 4.144 Å, corresponding to a Au-Au distance of 2.93 Å, in accord with Ref. 52. With the vacuum region set to 42.82 Å all calculations were performed in a 20.51 × 20.30 × 50.00 $Å^3$ simulation box under periodic boundary conditions (PBC) in all three directions. For the force-field calculations, a set of rigid-rod dipoles modelling the gold-surface electronic polarization and additional surface Lennard-Jones potentials were added using the default GolP-CHARMM settings [49, 50, 52]. The molecules were parameterized with the CHARMM General Force Field (CGenFF) [70, 71, 72, 73] (except water molecule for which the TIP3P model was used) and the atomic types were modified in accord with GolP-CHARMM. The same parameterization was used for the set of neutral amino acids of R-CH(NH_2)COOH molecular structure. Specific atom types and point charges used in the calculations can be found in the Supporting Information. The force-field simulations were performed in Gromacs 5.1.4 [74, 75] using the smooth particle mesh Ewald (PME) method [76, 77] with a cutoff of 9.5 Å and Lennard-Jones interactions that are smoothly switched off between 8.5 and 9.5 Å.

To find the adsorbed structure of each molecule we performed molecular dynamics (MD) simulations for 50 different initial structures per molecule. They were randomly rotated and placed into the vacuum region of the slab model while maintaining the shortest distance from the gold surface or its periodic image at a minimum of 5.0 Å. Whilst the gold-atom positions were frozen during the 100 ps long MD with 1 fs time step, the rigid-rod dipoles and the molecule were

free to move and their temperature was controlled by a Nose-Hoover thermostat [78, 79]. The dipole temperature was set to 300 K for the whole duration of the simulation while the molecular temperature continuously dropped from 300 K to 1 K between 20 and 80 ps of the run. The GolP-CHARMM adsorption energy of the final structure was evaluated by thermal sampling of the dipoles in the gold slab as well as the whole system, following the prescription from the original GolP work of Iori [49, 50]. Consistently with Ref. [52], the structure with the lowest adsorption energy was then compared with density-functional-theory (DFT) reference data. Other adsorbed structures were used to evaluate statistical mean and its standard deviation for adsorption energies and distances, which are presented in the Supporting Information.

Reference DFT calculations were performed with the CP2K software package [80] using the revised Perdew-Burke-Ernzerhof functional (revPBE) [66] with non-local correlation correction introducing dispersion interactions (revPBE-vdW known also as vdW-DF in literature) [67, 68, 69]. While the core electrons were described by Goedecker-Teter-Hutter (GTH) pseudopotentials [81], a triple-zeta (TZ) basis set from the CP2K database was used for gold and a double-zeta basis set with polarization functions (DZVP) for all other atoms. Fermi smearing with electronic temperature 300 K was applied to maintain fractional occupation numbers of metallic states near the Fermi level. A cut-off of 500 Ry was used to define the finest multi-grid used for real-space integration. The wavefunction was optimized to an accuracy of 10^{-6} a.u. For geometry optimization, several different adsorption structures obtained by GolP-CHARMM simulations (see above) were used as initial geometries, which were fully optimized by the limited-memory BFGS method [82] until changes in the atomic forces and in the root-mean-square atomic positions dropped below 10^{-4} a.u. The position of all gold atoms was frozen during the optimization. The molecular adsorption energy (E_{ads}) was obtained by subtracting the energy of

optimized isolated molecule (E_{mol}) and an isolated slab (E_{slab}) from the minimized energy of the slab with the molecule adsorbed (E_{sys}), $E_{ads} = E_{sys} - E_{mol} - E_{slab}$. The adsorption energy was corrected for basis-set superposition error (BSSE) using the counterpoise procedure [83] as implemented in CP2K.

III. Results and Discussion

III.1 Assessment of vdW density functionals

S22 database. As dispersion interaction is important for accurate structure prediction of organic molecules on metallic surfaces, we focused on DFT functionals with non-local correlation corrections (vdW-DF types [67, 68, 69, 84]). We compared the performance of three functionals, namely revPBE-vdW [66], used as a reference in Ref. [52], its optimized version optPBE [85, 86, 87] and a new second-generation rev-vdW-DF2 functional of Hamada [88, 89]. In a first series of calculations, we benchmarked the performance of these functionals on the S22 set of weakly-interacting molecular dimers [90]. We computed BSSE-corrected binding energies of the dimers in their original geometries obtained by accurate ab-initio methods and compared them with reference coupled-cluster values in the complete basis set limit (CCSD(T) / CBS) [91]. The mean unsigned errors (MUE, $\sum_n |y_{calc} - y_{ref}|/n$) of calculated energies using the DZVP basis set are 7.1, 1.8, and 3.5 kJ/mol for revPBE-vdW, optPBE-vdW and rev-vdW-DF2, respectively, which correspond to mean relative unsigned errors (MRUE, $\sum_n |y_{calc} - y_{ref}|/n|y_{ref}|$) of 24.6%, 8.4% and 16.5%. When we apply the larger TZV2PX basis set optimized for molecular calculations, the MRUEs reduce only slightly to 23.7%, 7.8% and 13.5% (cf. Fig. 1a). After full geometry optimization of the S22 pairs using the DZVP basis set, the root-mean-square deviation (RMSD)

of atom positions relative to CCSD(T) or MP2 reference structures is small, 0.11, 0.08 and 0.08 Å for revPBE-vdW, optPBE-vdW and rev-vdW-DF2, respectively. The MUEs in binding energy at the optimized geometries change to 3.9, 2.2 and 4.2 kJ/mol, respectively, corresponding to MRUEs of 13.3%, 12.0% and 13.5%. Thus, the performance of all three functionals is reasonably good with differences becoming less pronounced if consistent structures are used (cf. Fig. 1b).

Small molecules on gold. Next we calculated the adsorption energy of the molecules in the fitting set on Au(111) (see Computational Details for list of considered compounds). The outcome of these calculations is remarkably different with respect to the ones for the S22 database. While revPBE-vdW yields small MUEs of 3.4 kJ/mol compared to available experimental data (cf. Fig. 2 and Table S1 in Supporting Information) consistently with Ref. [52] where error of 3.7 kJ/mol was reported for the same functional, both optPBE-vdW and rev-vdW-DF2 functionals seem to over-bind the adsorbed structures leading to considerably higher MUE of 17.0 kJ/mol and 16.1 kJ/mol, respectively. In terms of relative errors, the functionals differ from experimental values on average by 6.4%, 32.7% and 30.0%. Obviously, the functionals which perform quite well for weakly bound molecules in the gas phase fail considerably for a molecule adsorbed on a highly-polarizable metal surface. Of course, the metal / organic interface is rather difficult for DFT because strongly delocalized electrons in metals are well described by the local-density approximation (LDA) while an accurate description of the varying electron density in molecular structures requires generalized gradient approximation (GGA), often supplemented with an admixture of Hartree-Fock exchange (HFX). The revPBE-vdW functional, as the first member or vdW-DF family, was derived from surface-science perspective using plasmon-based theory [84] and that is perhaps the reason why this functional provides a fairly accurate treatment of molecule / metal interactions, even reaching chemical accuracy for the set of molecules studied.

We find that the overbinding in optPBE-vdW and rev-vdW-DF2 functionals correlates with the trend in adsorption distances between the surface plane and the nearest heavy atom. These functionals predict systematically shorter adsorption distances than revPBE-vdW (3.6 – 3.7 Å for alkane chains, 3.1 – 3.4 Å for compounds containing double bonds, 2.8 – 3.0 Å for molecules interacting with gold via oxygen, ~ 2.9 Å for molecules with sulfur and ~2.5 Å for nitrogen-containing species), by 5.6% (optPBE-vdW) and even 9.5% (rev-vdW-DF2) on average. On the contrary, Wright *et al.* [52] argued that the revPBE-vdW distances are overestimated, but their argument is based on the gas phase behaviour discussed above, where the inter-molecular distances in optimized S22 pairs were found slightly longer than those obtained by accurate quantum-chemical methods. However, overestimation of adsorption distance in revPBE-vdW was reported also for azobenzene on Ag(111) surface [92] and PTCDA on Ag(111), Au(111) and Cu(111) [93, 94] where accurate experimental data are available from X-ray standing wave (XSW) measurements. Unfortunately, there are no such experimental adsorption structures available for the structures considered in this work, but judging from the good performance in adsorption energies, we believe that revPBE-vdW structures are more reliable compared to the other two functionals considered. The same conclusion was obtained for example by Rosa *et al.* [95] who investigated adsorption of benzene, ammonia and cytosine on Au(111) using different functionals from vdW-DF family.

With regard to the test set (see Computational Details for full list of structures), the relative performance of the considered DFT functionals is practically the same. However, the errors with respect to experimental reference data are somewhat larger. For adsorption energies, MUEs are 6.0, 23.4 and 23.7 kJ/mol for revPBE-vdW, optPBE-vdW and rev-vdW-DF2, respectively, which correspond to MRUEs 9.2%, 37.0% and 36.6%. The significant increase of

error is caused mainly by non-1-en and dibutylsulfid molecules, which are relatively long and adsorbed to the surface by specific site, i.e. double bond or sulfur atom. In both cases, the adsorption energy is lower in experiment than in DFT calculations. This suggests that the surface coverage might be somewhat higher on the real surfaces than in our model and the chains, interacting with their neighbours, are partly packed or tilted, which would lower their interaction energies. Structure uncertainties for these two molecules are also suggested by atypically large standard deviations of adsorption energies and distances (see Tables S1 and S3 in Supporting Information). When we omit these two compounds from the test set, the MRUEs drop to 7.1%, 29.6% and 28.3% for revPBE-vdW, optPBE-vdW and rev-vdW-DF2, respectively. These values and their trend are consistent with the results obtained before for the fitting set. Besides, the adsorption distances calculated for the test set molecules exhibit the same trend found for the fitting set, i.e. they are shortened by 6.6% and 10.9% for optPBE-vdW and rev-vdW-DF2 compared to revPBE-vdW. Therefore, due to its good predictive power, we decided to use revPBE-vdW as a reference DFT method for the calculation of amino acid adsorption energies, which are discussed in the next section.

III.2 GolP-CHARMM vs vdW-DF

Small molecules on gold. We applied the GolP-CHARMM force field in the Gromacs software package [74, 75] following the description in Ref. [52]. To validate our setup, we first investigate the performance of GolP-CHARMM for the small molecules in the fitting and test sets. The adsorption energies and distances are plotted against the revPBE-vdW reference values in Figs. 3 and 4 (see Tables S1 and S2 in Supporting Information for numerical values). The two sets yielded acceptable MUEs of 5.2 kJ/mol and 5.4 kJ/mol, respectively, corresponding to MRUEs of

11.8% and 10.5%. Similarly, the adsorption distances are in accord with the vdW-DF data with MUEs of 0.09 Å and 0.19 Å, corresponding to MRUEs of 3.1% and 6.4%, respectively. Small discrepancies with the original work of Wright et al. [52] are due to the use of different reference values (they refer to mixed experimental and DFT values while we use only vdW-DF data for consistency with the later discussion of neutral amino-acid adsorption for which no experimental data are available). Further differences could be caused by different point-charges on the molecular atoms, which we took from the CHARMM general force field for organic molecules (CGenFF).

In general, GolP-CHARMM well reproduces adsorption energies of the small molecules, however, it slightly underestimates the adsorption distances in most cases (however, revPBE-vdW reference data might have somewhat overestimated adsorption distances as we discuss above). The best agreement was found for the non-polar alkanes with MUEs only 2.9 kJ/mol and 0.03 Å. Unsaturated hydrocarbons containing double bonds perform are still well described (MUEs 4.8 kJ/mol and 0.07 Å), while to errors for aromatic benzene and toluene are larger (MUEs 9.8 kJ/mol and 0.05 Å). The trend of too short distances is more pronounced when heteroatoms are present. For example, oxygen-containing compounds such as methanol, acetone, formic acid and water exhibit together MUEs of 3.8 kJ/mol and 0.19 Å, while the molecules with nitrogen (methylamine, imidazole and ammonia) perform a bit worse in energy with MUEs 12.2 kJ/mol as well as in distancse (0.26 Å). Most importantly, from the perspective of this work, the molecules with sulfur show reasonably good MUE of 5.9 kJ/mol in adsorption energy, however, somewhat worse error in adsorption distance (0.30 Å). Both thiols (methanethiol, ethanethiols) and thioethers (diethylsulfide, dibutylsulfide) underestimate the adsorption distance by ~ 10% compared to the revPBE-vdW reference and tend to place the sulfur atom too close to the surface.

Neutral amino acids on gold. As in the case of small molecules discussed above we compare adsorption energies and structures of neutral amino acids predicted by GolP-CHARMM force field against reference DFT calculations. For the details regarding the generation of adsorption structures we refer to Section II. We note, that the DFT data presented here are for *neutral* amino acids (carboxyl and amine groups are not deprotonated or protonated as in solution) and thus correspond to vacuum surface adsorption without presence of water. With regard to the dispersion interaction included, the present DFT calculations are arguably the most accurate reported to date for the interaction of amino acids with gold. Although we used GolP-CHARMM structures as initial geometries for geometry optimizations in revPBE-vdW, we tested several initial configurations to find the most stable configuration for each amino acid. These are shown in Fig. S1 in the Supporting Information. All amino acids adsorb flat on the Au(111) surface. Typically, a neutral amino acid sticks to the gold surface by one of the groups containing electron-rich heteroatoms (nitrogen, oxygen or sulfur present in carboxyl, hydroxyl, amine, amide, thioether or thiol groups). Both carboxyl and amino groups attached to the alpha carbon are typically in close contact with the surface and so are the aromatic rings which exhibit significant stacking interaction. Sulfur atoms, either in form of thiol (Cys) or thioether (Met), always tends to be in direct contact with gold, as expected.

The GolP-CHARMM amino acid adsorption energies and distances are plotted against revPBE-vdW reference values in Fig. 5 (see Tables S3 and S4 in Supporting Information for numerical values). Overall, the MUE (MRUE) is 7.8 kJ/mol (11.3 %) and 0.26 Å (8.6 %). While the force field predicts the adsorption energies rather well, it systematically underestimates the adsorption distances (although the effect might be smaller because of probable overestimation of distance in reference revPBE-vdW data). We already observed this behaviour on the sets of small

molecules discussed above. Nevertheless, despite this discrepancy, we find that the minimum energy structures in the GolP-CHARMM force field and in revPBE-vdW are qualitatively rather similar. Comparing different groups of amino acids, the smallest errors with respect to revPBE-vdW data are observed for amides (Asn, Gln) with MUEs 1.5 kJ/mol and 0.08 Å while the corresponding carboxyl acids perform somewhat worse (MUEs 8.5 kJ/mol and 0.35 Å). Amines (Arg, Lys) exhibit the largest discrepancy with MUEs of 16.9 kJ/mol and 0.16 Å. Aliphatic (Ala, Gly, Ile, Leu, Pro, Val) and aromatic (His, Phe, Trp, Tyr) show reasonable error in the adsorption energy (8.7 kJ/mol and 4.7 kJ/mol, respectively) while the discrepancies in distances are rather large (0.32 Å and 0.25 Å, respectively), especially for the former ones. The amino acids with hydroxyl groups (Ser, Thr) perform quite well with errors of 3.4 kJ/mol and 0.22 Å. Finally, the sulfur-containing Met and Ser overbind with errors rising to 12.1 kJ/mol and 0.33 Å, in line with our observations for small molecules.

Sorting the amino acids according to decreasing adsorption energy (in absolute values), we obtain the following order: aromatic (-97.1 kJ/mol) > amines (-88.3 kJ/mol) > Cys, Met (-84.4 kJ/mol) > amides (-71.5 kJ/mol) > carboxylic (-70.5 kJ/mol) > aliphatic (-60.1 kJ/mol) > hydroxylic (-55.5 kJ/mol). Note that the general trend is in surprisingly good agreement with amino-acid adsorption on wetted Au(111)/water interface studied by Hoefling *et al.* [56] where the molecular side chains are charged and the overall structure and energetics is affected by interaction with solvation shell via network of hydrogen bonds. In general, the adsorption energy of a molecule, although often influenced by specific chemical groups, is mostly determined by its size, or more precisely, by the number of atoms in contact with the gold surface. Therefore, the adsorption energies of proteins cannot be obtained as a sum of amino-acid contributions as already pointed Nawrocki and Cieplak [58]. For better comparison, we normalized the data by

dividing the absolute adsorption energies by the number of heavy atoms in each amino acid. Then, the order is as follows: sulfur (-10.6 / -9.0) > amine (-8.0 / -9.6) ~ aliphatic (-8.1 / -7.9) ~ aromatic (-7.6 / -7.8) ~ amide (-7.5 / -7.5) ~ hydroxyl (-7.4 / -7.4) ~ carboxyl (-7.4 / -6.5), where the numbers in brackets are average contributions to the adsorption energy per heavy atoms in kJ/mol for GolP-CHARMM / vdW-DF, respectively. Indeed, except for the dominant sulfur-containing Cys and Met, the normalized adsorption energy is very similar for all amino acids with the absolute interaction strength determined by its size.

III.3. Parametrization of Au-S bonding

Parameters for covalent bonding of sulfur to gold surfaces were derived in several studies for different force fields. Hautman and Klein used a Lennard-Jones potential of the 12-3 form together with a Au-S harmonic bond of equilibrium distance r_0 = 2.4 Å and harmonic angle potential φ_0 = 100° to describe interaction of alkyl thiols with Au(111) [96]. Qian *et al.* used a series of 10-4 LJ potentials to describe the interaction between Au(111) and cyclodextrins in the Amber force field using the same harmonic bond potential as Hautman but no angular terms [35]. More recently, Bizzary *et al.* studied properties of chemisorbed plastocyanine on the gold surface using a CHARMM potential and the following harmonic potentials for interaction of cysteine sulfur with gold: Au-S bond: r_0 = 2.531 Å, k_r = 198 kcal/mol/Å^2; Au-S-C angle: φ_0 = 109°, k_φ = 46.347 kcal/mol/rad^2; Au-S-C-C dihedral angle: ϑ_0 = 180°, nk_ϑ= 0.312 kcal/mol [40]. Here, we report the bonding parameters for methanethiolate (H_3C-S-), thiocyanate (NC-S-) and cysteine thiolate (H_2N-CH(COOH)-S-) to Au(111) surface that are compatible with the polarizable GolP-CHARMM force field.

For a long time, there was some uncertainty about the preferred adsorption site of cysteine on flat Au(111) surface: *atop*, *bridge*, *hcp* hollow and *fcc* hollow sites are available, in principle (see Fig. S2 in Supporting Information). The *fcc* hollow site was found as the most preferred for methanethiolate at DFT(PBE) level of theory by Alexiadis *et al.* [97]. Cysteine-radical adsorption was studied by Di Felice *et al*. at GGA level (PW91 functional) in vacuum finding that the adsorption distances are the same, that is 2.51 Å, at *bridge* and *fcc* hollow sites and it is the *bridge* site which is energetically more stable [98]. Recently, Monti *et al*. [99] performed calculations based on the PBE functional to parameterize a reactive force field (ReaxFF) [100] for cysteine interaction with Au(111) surface. The optimal Au-S distance was found to be 2.4 Å and the activation barrier for hydrogen dissociation from SH to water solution was estimated to be ~10 kcal/mol from the MD simulations.

Here, we used the revPBE-vdW functional with dispersion that we have found to be the most suitable for adsorption of organic molecules on Au(111), as discussed above. In this functional, the *fcc* site, though very close in energy to the *hcp* site, is the most preferred adsorption position for methanethiolate. The potential energy curves are shown in Fig. 6 for all four sites where the adsorption distance was varied statically, i.e. without reoptimizing the molecular coordinates. The curves could be very well fitted to a Morse potential, $V(r) = D\left[1 - e^{-\alpha(r-r_0)}\right]^2$, where r_0 is the equilibrium distance (i.e. location of the potential minimum), α is a parameter controlling the curvature and D the dissociation energy or depth of the potential well. Numerical values of these parameters for the methanethiolate adsorption are listed in Table 1. It can be clearly seen that the shorter adsorption distances are associated with large adsorption energies (in absolute value). While the *atop* site is the least stable one with the adsorption distance ~ 2.7 Å and energy 52.8 kJ/mol, the hollow sites, slightly more preferred than

the bridge site, exhibit an adsorption distance of ~ 2.2 Å and energy of 122.1 kJ/mol (*fcc* site). Note that these locations are somewhat idealized considering upright position of the molecule perpendicular to the surface plane. Molecular tilting and further interaction with the surface usually shifts the adsorbed atom from the symmetric hollow site slightly closer to the bridge site. However, for our force-field fitting purposes, we consider only ideal upright adsorption to the *fcc* site.

We used three different sulfur-containing molecules for the fitting of Au-S interaction in the modified GolP-CHARMM force field. Methanethiolate (H_3C-S-) as a smallest model mimicking the biologically relevant Au-S bonding, thiocyanate (NC-S-) as a small model with different chemical character and cysteine thiolate (H_2N-CH(COOH)-S-), which is our main target bearing in mind applications on large biological systems. Potential energy curves of these systems are shown in Fig. 7 as obtained in revPBE-vdW and in GolP-CHARMM. Since methanethiolate and thiocyanate are symmetric molecules which interact with the surface only through the sulfur atom when they are adsorbed in upright position, their geometries were not reoptimized at different adsorption distances. On the other hand, structural changes with varying adsorption distance might be expected in case of cysteine thiolate, which is larger and contains several atoms close to the surface. Therefore, in this case we performed a relaxed potential-energy scan at revPBE-vdW level. We first optimized the adsorbed cysteine structure in upright position with carboxyl and amine groups pointing away from the surface and then we subsequently increased/decreased the adsorption distance and reoptimized the geometry constraining the Au-S distance. In total, 29 structures were evaluated for each molecule with the adsorption distance ranging from 1.5 to 5.0 Å.

To maintain sulfur adsorption to the surface via explicit bonding terms, we added three new atomic types to the GolP-CHARMM force field. These are used to create a surface binding site as it is shown in Fig. 8. In addition to standard bulk gold atoms (AUB type), surface gold atoms (AUS) with charged dipoles (AUC) and surface inter-atomic sites (AUI), we defined a charge-neutral gold atom type without dipole, termed AUA, and a inter-atomic site type, termed AUJ, which has a more shallow Lennard-Jones potential (ε = 0.10 kJ/mol, σ = 2.5 Å) than the original interatomic AUI site type (ε = 0.48 kJ/mol, σ = 3.8 Å). Finally, we created a dummy site type for the actual Au-S bonding, termed AUD. Obviously, these modifications are necessary to bring the adsorbed molecule in close contact with the surface, where direct interaction with surface dipoles is undesired, and anchor it to the *fcc* adsorption site. Lennard-Jones parameters of the AUJ sites are chosen in such a way that the binding potential-energy profiles of the studied molecules have minima close to the revPBE-vdW reference data and only a weak Au-S bonding term needs to be added to fit the potential curves well.

The revPBE-vdW potential curves are relatively well reproduced by the modified GolP-CHARMM force field containing the AUJ binding sites (compare 'vdW-DF' and 'GolP + LJ' curves in Fig. 7, even without adding the specific Au-S bonding term. Note that because of the different chemical nature the sulfur in thiocyanate, it is described by the standard CHARMM27 atomic type SS, while the sulfur in methanethiolate and cysteine is described by a ST atom type, introduced in GolP-CHARMM to capture the stronger interaction of gold surfaces with thiols. To further improve the agreement with the revPBE-vdW reference in the regions around the minima of the potential curves we added a Morse potential between the sulfur atom and the AUD dummy site located in the *fcc* hollow on the surface ('GolP + LJ + V_M' in Fig. 7). The optimized parameters are listed in Table 2 where we specify also the force constant of the corresponding

harmonic potential located at the same position and having the same curvature as the Morse potential ($k = 2\alpha^2 D$). As can be seen from the insets of Fig. 7, if GolP is supplemented with the harmonic (`GolP + LJ + V_H') rather than the Morse potentials, the potential is still well reproduced from the minimum up to several units of thermal energy at room temperature (~ 2.5 kJ/mol). Therefore, we suggest that the provided harmonic-potential parameters can be used for large-scale simulations without any significant loss of accuracy compared to Morse potentials.

Finally, we explored the angular dependence of the potential energy associated with the covalent Au-S bond. The methanethiolate and thiocyanate are symmetric molecules with the principal axes aligned to the surface normal in our model, however, in reality they adsorb on the Au(111) under a significant tilt angle. Therefore, we calculated the potential energy dependence on this angle in *atop* and *bridge* direction in revPBE-vdW and compared them with our modified GolP-CHARMM potential where the molecule was bound to the surface by the harmonic potential defined above. The resulting potential curves are shown in Fig. 9a and 9b. Indeed, the methanethiolate has the potential energy minimum at 45° while the thiocyanate prefers a somewhat larger tilting angle close to 60°. The GolP-CHARMM potential reproduces the general features of the potential curves, nevertheless, it exhibits a rather too shallow minimum in case of methanethiolate and overbinds the tilted structure of thiocyanate. In the latter case, the empirical potential tends to overestimate the tilting angle by 5-10° comparing to revPBE-vdW reference. Since cysteine does not have an axis of symmetry and the optimal adsorbed structure is not only tilted but it also interacts with the surface via carboxyl as well as amine groups, we rotated the molecule along the Au-S bond (i.e. surface normal direction) to explore the angular dependence in this case. The computed curve, shown in Fig. 9c, has several minima and maxima as the two hydrogens from the cysteine sidechain, which are the closest atoms to the gold surface except the

binding sulfur, feel the potential of surface atoms. Although the GolP-CHARMM curve is not as smooth as the vdW-DF reference due to fluctuating polarization effects, the position of the extrema and energy differences between them are relatively well reproduced. Therefore, we opted not to introduce any additional angular term into the force field and conclude that the chemisorption is satisfactorily described by the new surface binding-site LJ potentials and the Au-S bonding potential.

Conclusions

While in bioelectrochemistry one usually deals with *solvated* proteins attached to gold electrodes, in the emerging field of nanobioelectronics one is typically confronted with biomaterials interacting with metal electrodes under relatively dry or *vacuum* conditions. Simulations of biomolecules and their heterogeneous interfaces in vacuum are not (yet) very common and require careful validation of force fields that were primarily developed for aqueous phase applications in mind. Here, we tested the popular GolP-CHARMM force field for this purpose, which employs a rigid-rod dipole model to describe polarization of the metal. To provide reference data, we first carefully compared the performance of modern vdW-DF family of functionals with correlation corrections for dispersion. Based on these comparisons, we concluded that revPBE-vdW (i.e. the original vdW-DF) provides the best results for adsorption energies of organic molecules on gold surface, while it predicts reasonable accurate geometries for molecular dimers in vacuum. The GolP-CHARMM force field was then found to predict relatively accurate adsorption energies for neutral amino acids (mean unsigned error 7.8 kJ/mol, ~ 11.3 % compared to revPBE-vdW) while the adsorption distances tend to be underestimated (error 0.26 Å ~ 8.6 %).

Since in nanobioelectronic applications it is often important to immobilize peptides or proteins on the metal substrate, we report here how such chemisorption via Au-S bonding can be realized in the GolP-CHARMM force field. First, we confirmed by DFT that the *fcc* hollow site is preferred for attachment of sulfur to Au(111) surface and then we introduced new atom types in the force field to define such binding site. The potential energy profiles for the binding of three molecules (methanethiolate, thiocyanate and cysteine thiolate) were fitted to revPBE-vdW reference curves using Morse potentials, and in addition we provided parameters of harmonic potentials with the corresponding positions and curvatures, which we recommend for large-scale simulations of the heterogeneous interfaces with gold. In future work the augmented GolP-CHARMM force field will be used for the simulation of multi-heme proteins on Au(111), which were recently shown to exhibit unusually high currents [18].

Acknowledgements

Z. F. was supported by EPSRC Grant No. EP/M001946/1. J. B. acknowledges financial support from the European Research Council (ERC) under the European Union's Horizon 2020 research and innovation programme (grant agreement no. 682539/ SOFTCHARGE). Via our membership of the UK's HEC Materials Chemistry Consortium, which is funded by EPSRC (EP/L000202), this work used the ARCHER UK National Supercomputing Service (http://www.archer.ac.uk).

Supporting Information

Experimental and DFT values of adsorption energies and distances of small molecules; DFT optimized structures of neutral amino acids on the Au(111) surface; adsorption sites on Au(111) surface; parameterization of the small molecules and neutral amino acids in GolP-CHARMM force field; XYZ structures of small molecules and amino acids adsorbed on Au(111) surface.

References

(1) Davis, J. J.; Morgan, D. A.; Wrathmell, C. L.; Axford, D. N.; Zhao, J.; Wang, N.: Molecular Bioelectronics. *J. Mater. Chem.* **2005**, *15*, 2160-2174.

(2) Joachim, Ch.; Ratner, M. A.: Molecular Electronics: Some Views on Transport Junctions and Beyond. *Proc. Nat. Acad. Sci. U.S.A.* **2005**, *102*, 8801-8808.

(3) Nitzan, A.; Ratner, M. A.: Electron Transport in Molecular Wire Junctions. *Science* **2003**, *300*, 1384-1389.

(4) Adams, D. M.; Brus, L.; Chidsey, Ch. E. D.; Creager, S.; Creutz, C.; Kagan, C. R.; Kamat, P. V.; Lieberman, M.; Lindsay, S.; Marcus, R. A.; Metzger, R. M.; Michel-Beyerle, M. E.; Miller, J. R.; Newton, M. D.; Rolison, D. R.; Sankey, O.; Schanze, K. S.; Yardley, J.; Zhu. X.: Charge Transfer on the Nanoscale: Current Status. *J. Phys. Chem. B* **2003**, *107*, 6668-6697.

(5) Ruiz, M. P.; Aragones, A. C.; Camarero, N.; Vilhena, J. G.; Ortega, M.; Zotti, L. A.; Perez, R.; Cuevas, J. C.; Gorostiza, P.; Diez-Perez, I.: Bioengineering a Single-Protein Junction. *J. Am. Chem. Soc.* **2017**, *139*, 15337-15346.

(6) Park, H.; Lim, A. K. L.; Alivisatos, A. P. Park, J.; McEuen, P. L.: Fabrication of Metallic Electrodes with Nanometer Separation by Electromigration. *Appl. Phys. Lett.* **1999**, *75*, 301-303.

(7) Liu, K.; Avouris, Ph.; Bucchignano, J.; Martel, R.; Sun, S.; Michl, J.: Simple Fabrication Scheme for Sub-10 nm Electrode Gaps Using Electron-Beam Lithography. *Appl. Phys. Lett.* **2002**, *80*, 865-867.

(8) Bumm, L. A.; Arnold, J. J.; Cygan, M. T.; Dunbar, T. D.; Burgin, T. P.; Jones II, L.; Allara, D. L.; Tour, J. M.; Weiss, P. S.: Are Single Molecular Wires Conducting? *Science* **1996**, *271*, 1705-1707.

(9) Sakaguchi, H.; Hirai, A.; Iwata, F.; Sasaki, A.; Nagamura, T.; Kawata, E. Nakabayashi, S.: Determination of Performance on Tunnel Conduction through Molecular Wire Using a Conductive Atomic Foce Microscope. *Appl. Phys. Lett.* **2001**, *79*, 3708-3710.

(10) Smith, P. A.; Nordquist, Ch. D.; Jackson, T. N.; Mayer, T. S.; Martin, B. R.; Mbindyo, J.; Mallouk, T. E.: Electric-Field Assisted Assembly and Alignment of Metallic Nanowires. *Appl. Phys. Lett.* **2000**, *77*, 1399-1401.

(11) Freer, E. M.; Grachev, O.; Duan, X.; Martin, S.; Stumbo, D. P.: High-Yield Self-Limiting Single-Nanowire Assembly with Dielectrophoresis. *Nat. Nanotech.* **2010**, *5*, 525-530.

(12) Noy, G.; Ophir, A.; Selzer, Y.: Response of Molecular Junctions to Surface Plasmon Polaritons. *Angew. Chem. Int. Ed.* **2010**, *49*, 5734-5736.

(13) Ron, I.; Pecht, I. Sheves, M.; Cahen, D.: Proteins as Solid-State Electronic Conductors. *Acc. Chem. Res.* **2010**, *43*, 945-953.

(14) Amdursky, N.; Marchak, D.; Sepunaru, L.; Pecht, I.; Sheves, M.; Cahen, D.: Electronic Transport via Proteins. *Adv. Mater.* **2014**, *26*, 7142-7161.

(15) Kumar, K. S.; Pasula, R. R.; Lim, S.; Nijhuis, Ch. A.: Long-Range Tunneling Processes across Ferritin-Based Junctions. *Adv. Mater.* **2015**, *28*, 1824-1830.

(16) Yu, X.; Lovrincic, R.; Sepunaru, L.; Li, W.; Vilan, A.; Pecht, I.; Sheves, M.; Cahen, D.: Insights into Solid-State Electron Transport through Proteins from Inelastic Tunneling Spectroscopy: The Case of Azurin. *ACS Nano* **2015**, *9*, 9955-9963.

(17) Fereiro, J. A.; Yu, X.; Pecht, I.; Sheves, M.; Cueas, J. C.; Cahen, D.: Tunneling Explains Efficient Electron Transport via Protein Junctions. *Proc. Natl. Acad. Sci. U.S.A.* **2018**, *115*, 4577-4583.

(18) Garg, K.; Ghosh, M.; Eliash, T.; van Wonderen, J. H.; Butt, J. N.; Shi, L.; Jiang, X.; Futera, Z.; Blumberger, J.; Pecht, I.; Sheves, M.; Cahen, D.: Direct Evidence for Heme-Assisted Solid-State Electronic Conduction in Multi-Heme c-Type Cytochromes. *Chem. Sci.* **2018**, DOI: 10.1039/C8SC01716F.

(19) Breuer, M.; Rosso, K. M.; Blumberger, J.; Butt, J. N.: Multi-Haem Cytochromes in *Shewanella oneidensis* MR-1: Structures, Functions and Opportunities. *J. R. Soc. Interface* **2015**, *12*, 20141117.

(20) Blumberger, J.: Recent Advances in the Theory and Molecular Simulation of Biological Electron Transfer Reactions. *Chem. Rev.* **2015**, *115*, 11191-11238.

(21) Jiang, X.; Futera, Z.; Ali, Md. E.; Gajdos, F.; von Rudorff, G. F.; Carof, A.; Breuer, M.; Blumberger, J.: Cysteine Linkages Accelerate Electron Flow through Tetra-Heme Protein STC. *J. Am. Chem. Soc.* **2017**, *139*, 17237-17240.

(22) Blumberger, J.: Electron Transfer and Transport through Multi-Heme Proteins: Recent Progress and Future Directions. *Curr. Opin. Chem. Biol.* **2018**, *47*, 24-31.

(23) Elliott, M.; Dafydd, J.: Approaches to Single-Molecule Studies of Metalloprotein Electron Transfer Using Scanning Probe-Based Techniques. *Biochem. Soc. Trans.* **2018**, *46*, 1-9.

(24) Gaigalas, A. K.; Niaura, G.: Measurement of Electron Transfer Rates between Adsorbed Azurin and a Gold Electrode Modified with a Hexanethiol Layer. *J. Coll. Interface Sci.* **1997**, *193*, 60-70.

(25) Chi, Q.; Zhang, J.; Nielsen, J. U.; Friis, E. P.; Chorkendorff, I.; Canters, G. W.; Andersen, J. E. T.; Ulstrup, J.: Molecular Monolayers and Interfacial Electron Transfer of *Pseudomonas aeruginosa* Azurin on Au(111). *J. Am. Chem. Soc.* **2000**, *122*, 4047-4055.

(26) Khoshtariya, D. E.; Dolidze, T. D.; Shushanyan, M.; Davis, K. L.; Waldeck, D. H.; van Eldik, R.: Fundamental Signatures of Short- and Long-Range Electron Transfer for the Blue Copper Protein Azurin at Au/SAM Junctions. *Proc. Natl. Acad. Sci. U.S.A.* **2010**, *107*, 2757-2762.

(27) Baldacchini, C.; Bizzarri, A. R.; Cannistraro, S.: Electron Transfer, Conduction and Biorecognition Properties of the Redox Metalloprotein Azurin Assembled onto Inorganic Substrates. *Eur. Polym. J.* **2016**, *83*, 407-427.

(28) Khoshtariya, D. E.; Wei, J.; Li, H.; Yue, H.; Waldeck, D. H.: Charge-Transfer Mechanism for Cytochrome c Adsorbed on Nanometer Thick Films. Distinguishing Frictional Control from Conformational Gating. *J. Am. Chem. Soc.* **2003**, *125*, 7704-7714.

(29) Morimoto, J.; Tanaka, H.; Kawai, T.: Direct Measurement of Electron Transport Features in Cytochrome c via V-I Characteristics of STM Currents. *Surf. Sci.* **2005**, *580*, L103-L108.

(30) Yue, H.; Khoshtariya, D.; Waldeck, D. H.; Grochol, J.; Hildebrandt, P.; Murgida, D. H.: On the Electron Transfer Mechanism Between Cytochrome c and Metal Electrodes. Evidence for Dynamic Control at Short Distances. *J. Phys. Chem. B* **2006**, *110*, 19906-19913.

(31) Davis, J. J.; Peters, B.; Wang, X.: Force Modulation and Electrochemical Gating of Conductance in a Cytochrome. *J. Phys.: Condens. Matter* **2008**, *20*, 374123.

(32) Amdursky, N.; Ferber, D.; Bortolotti, C. A.; Dolgikh, D. A.; Chertkova, R. V.; Pecht, I.; Sheves, M.; Cahen, D.: Solid-State Electron Transport via Cytochrome c Depends on

Electronic Coupling to Electrodes and Across the Protein. *Proc. Natl. Acad. Sci. U.S.A.* **2014**, *111*, 5556-5561.

(33) Gerster, D.; Reichert, J.; Bi, H.; Barth, J. V.; Kaniber, S. M.; Holleitner, A. W.; Visoly-Fisher, I.; Sergani, S.; Carmeli, I.: Photocurrent of a Single Photosynthetic Protein. *Nat. Nanotech.* **2012**, *7*, 673-676.

(34) Yu, J.; Becker, M. L.; Carri, G. A. Limited Growth Mechanism of Peptide-Mediated Gold-Nanoparticle Synthesis. *Small* **2010**, *20*, 2242-2245.

(35) Qian, J.; Hentschke, R.; Knoll, W.: Superstructures of Cyclodextrin Derivatives on Au(111): A Combined Random Planting-Molecular Dynamics Approach. *Langmuir* **1997**, *13*, 7092-7098.

(36) Braun, R.; Sarikaya, M.; Schulten, K.: Genetically Engineered Gold-Binding Polypeptides: Structure Prediction and Molecular Dynamics. *J. Biomat. Sci.* **2002**, *13*, 747-757.

(37) Feng, J.; Pandey, R. B.; Berry, R. J.; Farmer, B. L.; Naik, R. R.; Heinz, H. Adsorption Mechanism of Single Amino Acid and Surfactant Molecules to Au {111} Surfaces in Aqueous Solution: Design Rules for Metal-Binding Molecules. *Soft Matter* **2011**, *7*, 2113-2120.

(38) Verde, A. V.; Acres, J. M.; Maranas, J. K. Investigating the Specificity of Peptide Adsorption on Gold Using Molecular Dynamics Simulations. *Biomacromolecules* **2009**, *10*, 2118-2128.

(39) Verde, A. V.; Beltramo, P. J.; Maranas, J. K. Adsorption of Homopolypeptides on Gold Investigated Using Atomistic Molecular Dynamics. *Lagnmuir* **2011**, *27*, 5918-5926.

(40) Bizzarri, A. R.; Bonanni, B.; Constantini, G.; Cannistrato, S.: A Combined Atomic Force Microscopy and Molecular Dynamics Simulation Study on a Plastocyanin Mutant Chemisorbed on a Gold Surface. *ChemPhysChem* **2003**, *4*, 1189-1195.

(41) Heinz, H.; Farmer, B. L.; Pandey, R. B.; Slocik, J. M.; Patnaik, S. S.; Pachter, R.; Naik, R. R. Nature of Molecular Interactions of Peptides with Gold, Palladium, and Pd-Au Bimetal Surfaces in Aqueous Solution. *J. Am. Chem. Soc.* **2009**, *131*, 9704-9714.

(42) Heinz, H.; Vaia, R. A.; Farmer, B. L.; Naik, R. R.: Accurate Simulation of Surface and Interfaces of Face-Centered Cubic Metals Using 12-6 and 9-6 Lennard-Jones Potentials. *J. Phys. Chem. C* **2008**, *112*, 17281-17290.

(43) Heinz, H.; Lin, T.-J.; Mishra, R. K.; Emami, F. S.: Thermodynamically Consistent Force Fields for the Assembly of Inorganic, Organic, and Biological Nanostructures: The INTERFACE Force Field. *Langmuir* **2013**, *29*, 1754-1765.

(44) Heinz, H.; Jha, K. C.; Luettmer-Strathmann, J.; Farmer, B. L.; Naik, R. R. Polarization at Metal-Biomolecular Interfaces in Solution. *J. R. Soc. Interface* **2011**, *8*, 220-232.

(45) Finnis, M. W.: The Interaction of a Point Charge with an Aluminium (111) Surface. *Surf. Sci.* **1991**, *241*, 61-72.

(46) Finnis, M. W.; Kaschner, R.; Kruse, C.; Furthmuller, J.; Scheffler, M.: The Interaction of a Point Charge with a Metal Surface: Theory and Calculations for (111), (100) and (110) Aluminium Surfaces. *J. Phys.: Condens. Matter* **1995**, *7*, 2001-2019.

(47) Tarmyshov, K. B.; Muller-Plathe, F.: Interface between Platinum (111) and Liquid Isopropanol (2-Propanol): A Model for Molecular Dynamics Studies. *J. Chem. Phys.* **2007**, *126*, 074702.

(48) Siepmann, J. I.; Sprik, M.: Influence of Surface Topology and Electrostatic Potential on Water/Electrode Systems. *J. Phys. Chem.* **1995**, *102*, 511-524.

(49) Iori, F.; Corni, S.: Including Image Charge Effects in the Molecular Dynamics Simulations of Molecules on Metal Surfaces. *J. Comput. Chem.* **2008**, *29*, 1656-1666.

(50) Iori, F.; Di Felice, R.; Molinari, E.; Corni, S.: GolP: An Atomistic Force-Field to Describe the Interaction of Proteins With Au(111) Surfaces in Water. *J. Comput. Chem.* **2009**, *30*, 1465-1476.

(51) Dick, B. G., Jr.; Overhauser, A. W.: Theory of the Dielectric Constants of Alkali Halide Crystals. *Phys. Rev.* **1958**, *112*, 90-103.

(52) Wright, L. B.; Rodger, P. M.; Corni, S.; Walsh, T. R.: GolP-CHARMM: First-Principles Based Force Fields for the Interaction of Proteins with Au(111) and Au(100). *J. Chem. Theory Comput.* **2013**, *9*, 1616-1630.

(53) Jorgensen, W. L.; Maxwell, D. S.; Tirado-Rives, J.: Development and Testing of the OPLS All-Atom Force Field on Conformational Energetics and Properties of Organic Liquids. *J. Am. Chem. Soc.* **1996**, *118*, 11225-11236.

(54) Kaminski, G. A.; Friesner, R. A.; Tirado-Rives, J.; Jorgensen, W. L.: Evaluation and Reparametrization of the OPLS-AA Force Field for Proteins via Comparison with Accurate Quantum Chemical Calculations on Peptides. *J. Phys. Chem. B* **2001**, *105*, 6474-6487.

(55) Golze, D.; Iannuzzi, M.; Ngyuen, M.-T.; Passerone, D.; Hutter, J.: Simulation of Adsorption Processes at Metallic Interfaces: An Image Charge Augmented QM/MM Approach. *J. Chem. Theory Comput.* **2013**, *9*, 5086-5097.

(56) Hoefling, M.; Iori, F.; Corni, S.; Gottschalk, K.-E. Interaction of Amino Acids with the Au(111) Surface: Adsoption Free Energies from Molecular Dynamics Simulations. *Langmuir* **2010**, *26*, 8347-8351.

(57) Feng, J.; Slocik, J. M.; Sarikaya, M.; Naik, R. R.; Farmer, B. L.; Heinz, H. Influence of the Shape of Nanostructured Metal Surfaces on Adsorption of Single Peptide Molecules in Aqueous Solution. *Small* **2012**, *8*, 1049-1059.

(58) Nawrocki, G.; Cieplak, M.: Aqueous Amino Acids and Proteins Near the Surface of Gold in Hydrophilic and Hydrophobic Force Fields. *J. Phys. Chem. C* **2014**, *118*, 12929-12943.

(59) Hong, G.; Heinz, H.; Naik, R. R.; Farmer, B. L.; Pachter, R.: Toward Understanding Amino Acid Adsorption at Metallic Interfaces: A Density Functional Theory Study. *ACS Appl. Mater. Interfaces* **2009**, *1*, 388-392.

(60) Ghiringhelli, L. M.; Site, L. D.: Phenylalanine Near Inorganic Surfaces: Conformational Statistics vs Specific Chemistry. *J. Am. Chem. Soc.* **2008**, *130*, 2634-2638.

(61) Hoefling, M.; Iori, F.; Corni, S.; Gottschalk, K.-E. The Conformations of Amino Acids on a Gold(111) Surface. *ChemPhysChem* **2010**, *11*, 1763-1767.

(62) Yu, J.; Becker, M. L.; Carri, G. A. The Influence of Amino Acid Sequence and Functionality on the Binding Process of Peptides onto Gold Surfaces. *Langmuir* **2012**, *28*, 1408-1417.

(63) Siwko, M.; Corni, S.: Cytochrome c on a Gold Surface: Investigating Structural Relaxations and Their Role in Protein-Surface Electron Transfer by Molecular Dynamics Simulations. *Phys. Chem. Chem. Phys.* **2013**, *15*, 5945-5956.

(64) Peng, C.; Liu, J.; Zhou, J.: Molecular Simulations of Cytochrome c Adsorption on a Bare Gold Surface: Insight for the Hindrance of Electron Transfer. *J. Phys. Chem. C* **2015**, *119*, 20773-20781.

(65) Bortolotti, C. A.; Borsari, M.; Sola, M.; Chertkova, R.; Dolgikh, D.; Kotlyar, A.; Facci, P.: Orientation-Dependent Kinetics of Heterogeneous Electron Transfer for Cytochrome c Immobilized on Gold: Electrochemical Determination and Theoretical Prediction. *J. Phys. Chem. C.* **2007**, *111*, 12100-12105.

(66) Hammer, B.; Hansen, L. B.; Norskov, J. K.: Improved Adsorption Energies within Density-Functional Theory Using Revised Perdew-Burke-Ernzerhof Functionals. *Phys. Rev. B* **1999**, *59*, 7413-7421.

(67) Dion, M.; Rydberg, H.; Schroder, E.; Langreth, D. C.; Lundqvist, B. I.: Van der Waals Density Functional for General Geometries. *Phys. Rev. Lett.* **2004**, *92*, 246401.

(68) Thonhauser, T.; Cooper, V. R.; Li, S.; Puzder, A.; Hyldgaard, P.; Langreth, D. C.: Van der Waals Density Functional: Self-Consistent Potential and the Nature of the van der Waals Bond. *Phys. Rev. B* **2007**, *76*, 125112.

(69) Roman-Perez, G.; Soler, J. M.: Efficient Implementation of a van der Waals Density Functional: Application to Double-Wall Carbon Nanotubes. *Phys. Rev. Lett.* **2009**, *103*, 96102.

(70) Vanommeslaeghe, K.; Hatcher, E.; Acharya, C.; Kundu, S.; Zhong, S.; Shim, J.; Darian, E.; Guvench, O.; Lopes, P.; Vorobyov, I.; MacKerell, A. D., Jr.: CHARMM General Force Field: A Force for Drug-Like Molecules Compatible with the CHARMM All-Atom Additive Biological Force Fields. *J. Comput. Chem.* **2010**, *31*, 671-690.

(71) Yu, W.; He, X.; Vanommeslaeghe, K.; MacKerell, A. D., Jr.: Extension of the CHARMM General Force Field to Sulfonyl-Containing Compounds and Its Utility in Biomolecular Simulations. *J. Comput. Chem.* **2012**, *33*, 2451-2468.

(72) Vanommeslaeghe, K.; MacKerell, A. D., Jr.: Automation of the CHARMM General Force Field (CGenFF) I: Bond Perception and Atom Typing. *J. Chem. Info. Model.* **2012**, *52*, 3144-3154.

(73) Vanommeslaeghe, K.; Raman, E. P.; MacKerell, A. D., Jr.: Automation of the CHARMM General Force Field (CGenFF) II: Assignment of Bonded Parameters and Partial Atomic Charges. *J. Chem. Info. Model.* **2012**, *52,* 3155-3168.

(74) Berendsen, H. J. C.; van der Spoel, D.; van Drunen, R.: GROMACS: A Message-Passing Parallel Molecular Dynamics Implementation. *Comput. Phys. Comm.* **1995**, *91*, 43-56.

(75) Abraham, M. J.; van der Spoel, D.; Lindahl, E.; Hess, B.: GROMACS User Manual version 5.1.4, www.gromacs.org, **2016**.

(76) Darden, T.; York, D.; Pedersen, L.: Particle Mesh Ewald: An N log N Method for Ewald Sums in Large Systems. *J. Chem. Phys.* **1993**, *98*, 10089-10092.

(77) Essmann, U.; Perena, L.; Berkowitz, M. L.; Darden, T.; Lee, H.; Pedersen, L. G.: A Smooth Particle Mesh Ewald Method. *J. Chem. Phys.* **1995**, *103*, 8577-8593.

(78) Nose, S.: A Unified Formulation of the Constant Temperature Molecular Dynamics Methods. *J. Chem. Phys.* **1984**, *81*, 511-519

(79) Hoover, W. G.: Canonical Dynamics: Equilibrium Phase-Space Distributions. *Phys. Rev. A: At., Mol., Opt. Phys.* **1985**, *31*, 1695-1697.

(80) Hutter, J.; Iannuzzi, M.; Schiffmann, F.; VandeVondele, J.: CP2K: Atomistic Simulations of Condensed Matter System. *WIREs Comput. Mol. Sci.* **2014**, *4*, 15-25.

(81) Goedecker, S.; Teter, M.; Hutter, J.: Separable Dual-Space Gaussian Pseudopotentials. *Phys. Rev. B. Condens. Matter Mater. Phys.* **1996**, *54*, 1703-1710.

(82) Byrd, R. H.; Lu, P.; Nocedal, J.; Zhu, C.: A Limited Memory Algorithm for Bound Constrained Optimization. *SIAM J. Sci. Comput.* **1995**, *16*, 1190-1208.

(83) Boys, S. F.; Bernardi, F.: The Calculation of Small Molecular Interactions by the Differences of Separate Total Energies. Some Procedures with Reduced Errors. *Mol. Phys.* **1970**, *19*, 533-566.

(84) Berland, K.; Cooper, V. R.; Lee, K.; Schroder, E.; Thonhauser, T.; Hyldgaard, P.; Lundqvist, B. I.: van der Waals Forces in Density Functional Theory: A Review of the vdw-DF Method. *Rep. Prog. Phys.* **2015**, *78*, 066501.

(85) Klimes, J.; Bowler, D. R.; Michaelides, A.: Chemical Accuracy for the van der Waals Density Functional. *J. Phys.: Condens. Matter* **2010**, *22*, 022201.

(86) Klimes, J.; Bowler, D. R.; Michaelides, A.: Van der Waals density Functionals Applied to Solids. *Phys. Rev. B* **2011**, *83*, 195131.

(87) Carrasco, J.; Klimes, J.; Michaelides, A.: The Role of van der Waals Forces in Water Adsorption on Metals. *J. Chem. Phys.* **2013**, *138*, 024708.

(88) Hamada, I.: van der Waals Density Functional Made Accurate. *Phys. Rev. B* **2014**, *89*, 121103.

(89) Callsen, M.; Hamada, I.: Assessing the Accuracy of the van der Waals Density Functionals for Rare-Gas and Small Molecular Systems. *Phys. Rev. B* **2015**, *91*, 195103.

(90) Jurecka, P.; Sponer, J.; Cerny, J.; Hobza, P.: Benchmark Database of Accurate (MP2 and CCSD(T) Complete Basis Set Limit) Interaction Energies of Small Model Complexes, DNA Base Pairs, and Amino Acid Pairs. *Phys. Chem. Chem. Phys.* **2006**, *8*, 1985-1993.

(91) Takatani, T.; Hohenstein, E. G.; Malagoli, M.; Marshall, M. S.; Sherrill, C. D.: Basis Set Consistent Revision of the S22 Test Set of Noncovalent Energies. *J. Chem. Phys.* **2010**, *132*, 144104.

(92) Li, G.; Tamblyn, I.; Cooper, V. R.; Gao, H.-J.; Neaton, J. B.: Molecular Adsorption on Metal Surfaces with van der Waals Density Functionals. *Phys. Rev. B* **2012**, *85*, 121409.

(93) Romaner, L.; Nabok, D.; Puschnig, P.; Zojer, E.; Ambrosch-Draxl, C.: Theoretical Study of PTCDA Adsorbed on the Coinage Metal Surfaces, Ag(111), Au(111) and Cu(111). *New. J. Phys.* **2009**, *11*, 053010.

(94) Ruiz, V. G.; Liu, W.; Zojer, E.; Scheffler, M.; Tkatchenko, A.: Density-Functional Theory with Screened van der Waals Interactions for the Modeling of Hybrid-Inorganic Systems. *Phys. Rev. Lett.* **2012**, *108*, 146103.

(95) Rosa, M.; Corni, S.; Di Felice, R.: van der Waals Effects at Molecule-Metal Interfaces. *Phys. Rev. B* **2014**, *90*, 125448.

(96) Hautman, J.; Klein, M. L.: Simulation of a Monolayer of Alkyl Thiol Chains. *J. Chem. Phys.* **1989**, *91*, 4994-5001.

(97) Alexiadis, O.; Harmandaris, V. A.; Mavrantzas, V. G.; Site, L. D.: Atomistic Simulation of Alkanethiol Self-Assembled Monolayers on Different Metal Surfaces via a Quantum, First-Principles Parametrization of the Sulfur-Metal Interaction. *J. Phys. Chem. C* **2007**, *111*, 6380-6391.

(98) Di Felice, R.; Selloni, A.; Molinari, E.: DFT Study of Cysteine Adsorption on Au(111). *J. Phys. Chem. B* **2003**, *107*, 1151-1156.

(99) Monti, S.; Carravetta, V.; Agren, H.: Simulation of Gold Functionalization with Cysteine by Reactive Molecular Dynamics. *J. Phys. Chem. Lett.* **2016**, *7*, 272-276.

(100) van Duin, A. C. T.; Dasgupta, S.; Lorant, F.; Goddard, W. A., III: ReaxFF: A Reactive Force Field for Hydrocarbons. *J. Phys. Chem. A.* **2001**, *105*, 9396-9409.

Tables and Figures

Site	r_0	α	D
atop	2.715	1.334	52.773
bridge	2.269	1.262	101.901
fcc	2.187	1.133	122.118
hcp	2.194	1.146	118.558

Table 1: Parameters of the Morse potential as fitted to the revPBE-vdW potential energy curve of methanethiolate with respect to the distance from the Au(111) surface: equilibrium distance r_0 [Å], exponential factor α [$Å^{-1}$] and dissociation energy D [kJ/mol].

Molecule	r_0	k	α	D
Methanethiolate	2.567	77.138	0.562	122.180
Thiocyanate	2.429	1.727	0.105	78.519
Cysteine	1.842	19.624	0.573	29.914

Table 2: Parameters of the harmonic and Morse potentials as fitted to the revPBE-vdW potential energy surface: equilibrium distance r_0 [Å], harmonic force constant k [kJ/mol/$Å^2$], Morse exponential factor α [$Å^{-1}$] and Morse dissociation energy D [kJ/mol].

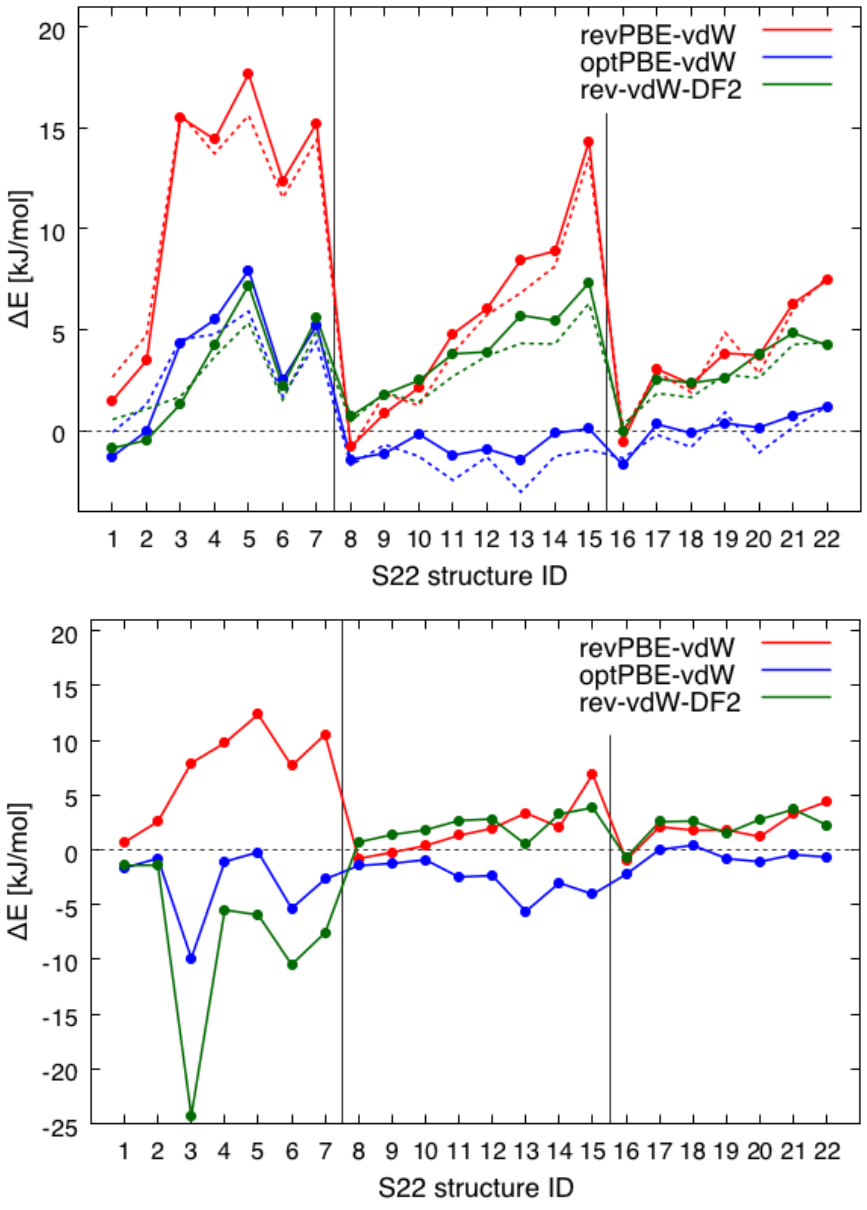

Figure 1: Deviation of DFT binding energies of S22 dimers with respect to ab initio values from Ref. 91. The binding energies were evaluated (a) on original S22 structures from Ref. 90 (solid lines: DZVP basis set, dashed lines: TZV2PX-Mol basis set) and (b) on DFT optimized structures. The vertical lines mark blocks of hydrogen-bonded complexes (1-7), complexes with predominant dispersion contribution (8-15) and complexes with mixed hydrogen-bonding and dispersion (16-22).

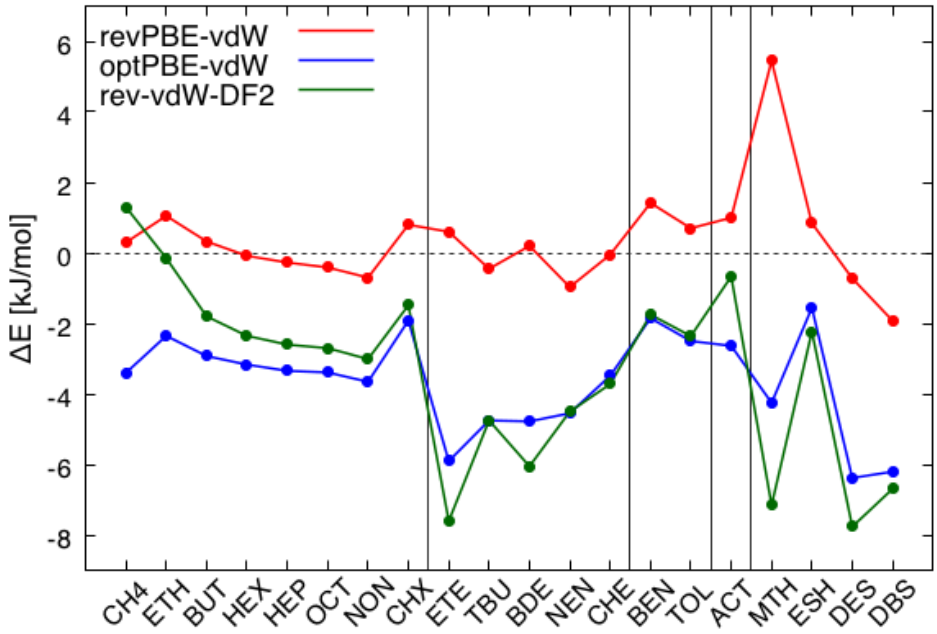

Figure 2: Deviation of DFT adsorption energies of small molecules on Au(111) surface with respect to experimental values (cf. Table S1 in Supporting Information). The energies are divided by the number of heavy atoms in the molecule. The vertical lines mark blocks of (cyclo)alkane molecules with single bonds, molecules with doubles, aromatic molecules, molecules with oxygen and molecules with sulfur, respectively.

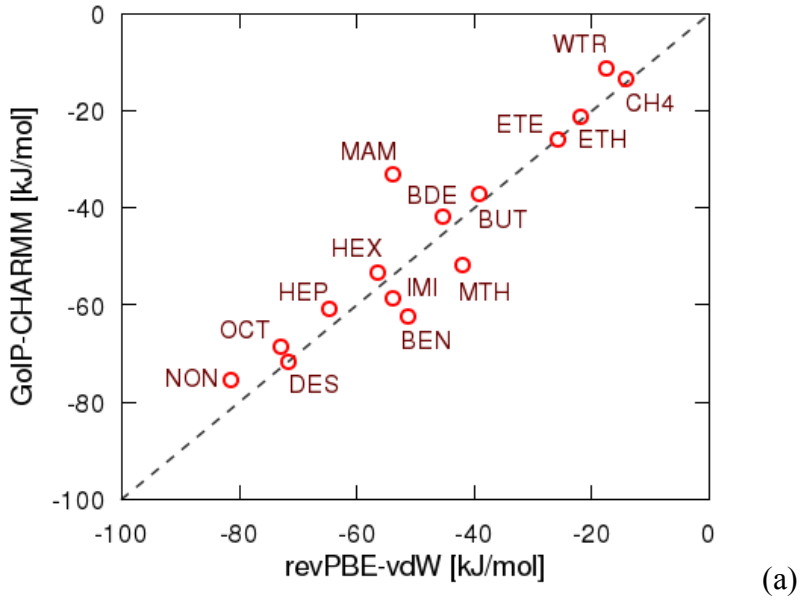

(a)

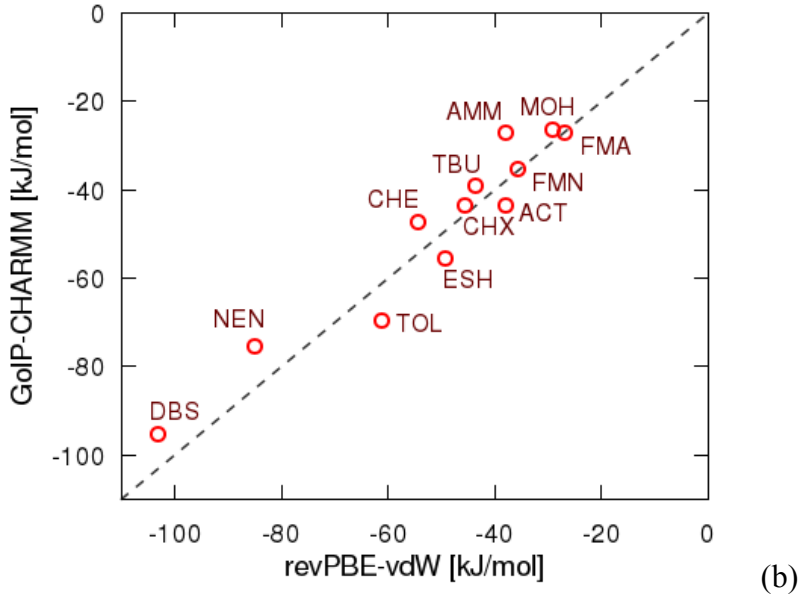

(b)

Figure 3: Correlation of adsorption energies [kJ/mol] obtained from the GolP-CHARMM force field and revPBE-vdW DFT reference data for (a) the fitting set and (b) the test set of small molecules used in Ref. 52.

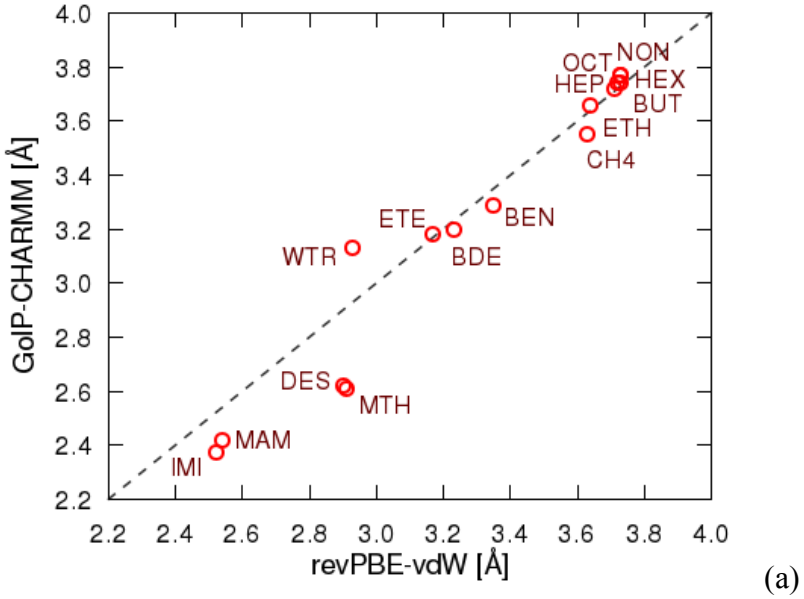

Figure 4: Correlation of adsorption distances [Å] obtained from GolP-CHARMM force field and revPBE-vdW DFT reference data for (a) the fitting set and (b) the test set of small molecules used in Ref. 52.

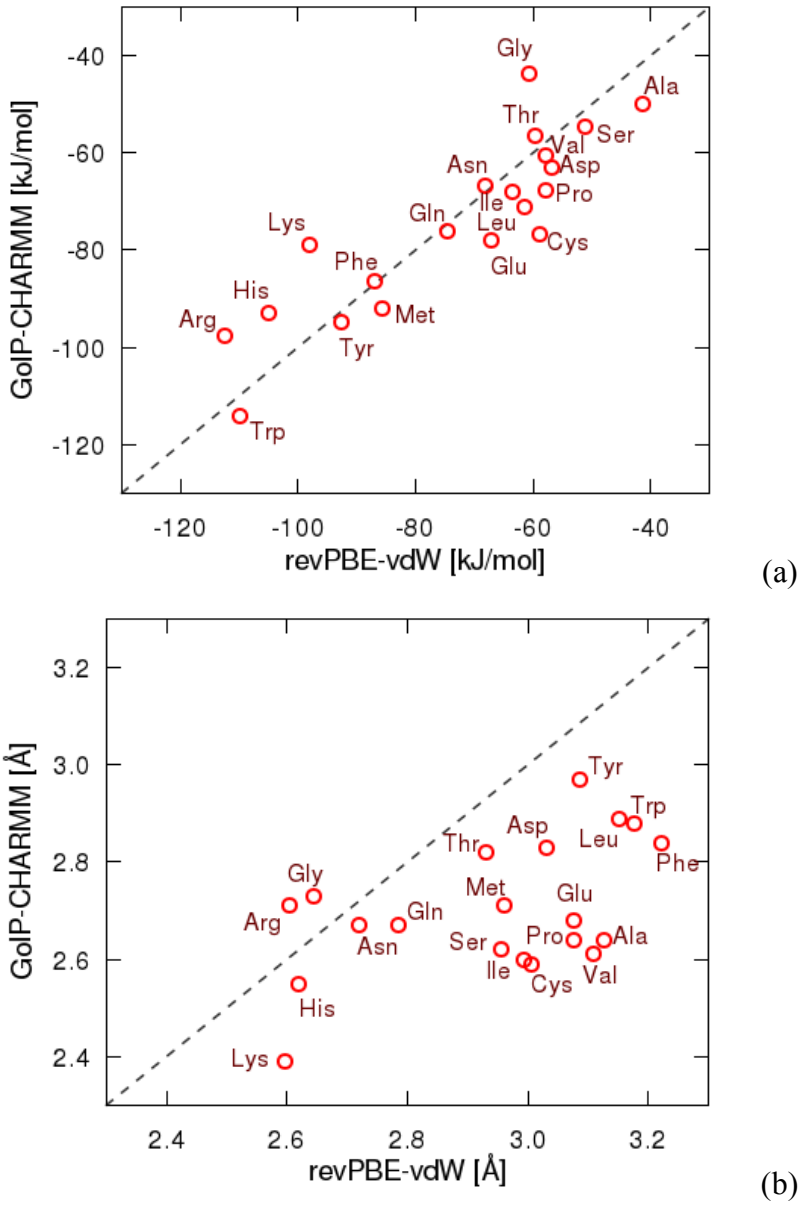

Figure 5: Correlation of amino acid (a) adsorption energies [kJ/mol] and (b) adsorption distances [Å] obtained with the GolP-CHARMM force field and revPBE-vdW DFT reference data.

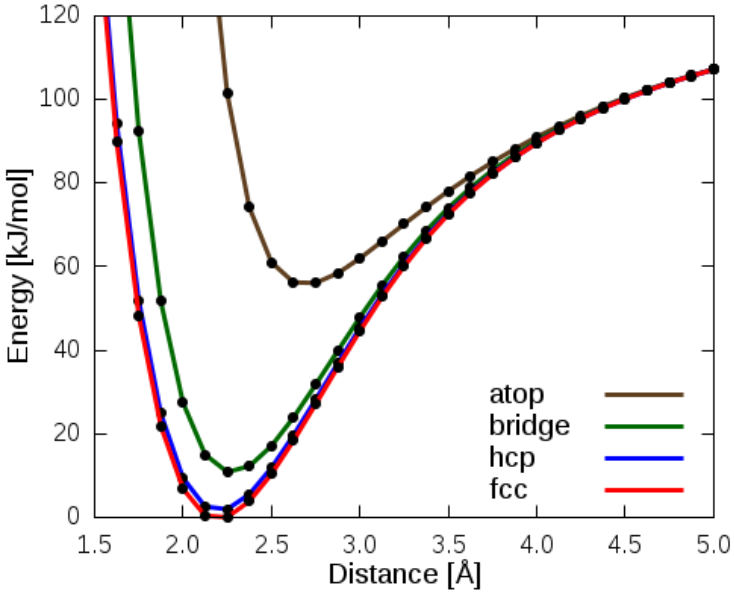

Figure 6: Potential energy vs Au-S distance for methanethiolate (CH_3-S-) adsorbed on *atop*, *bridge*, *hpc* hollow or *fcc* hollow sites of Au(111). The potential energy was obtained at revPBE-vdW level of theory.

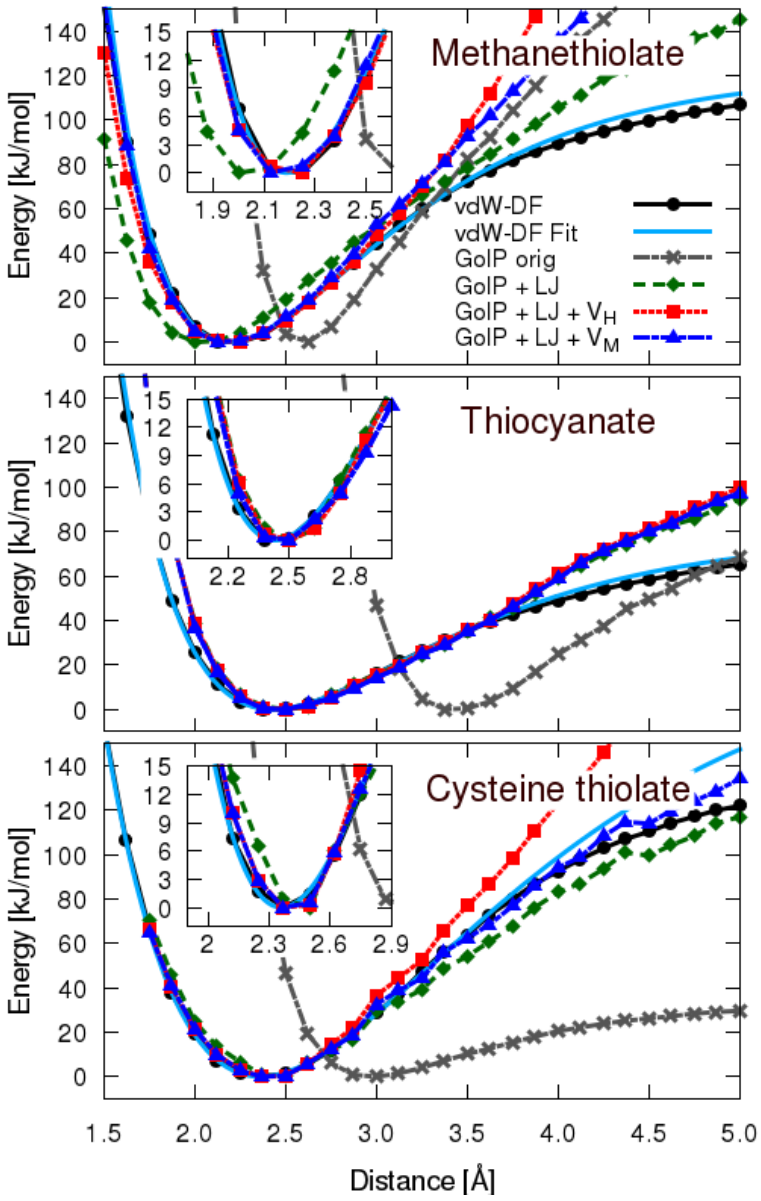

Figure 7: Potential energy curves along the Au-S bond for the fcc adsorption site of Au(111) for methanethiolate (H_3C-S-), thiocyanate (NC-S-) and cysteine thiolate (H_2N-CH(COOH)-S-). The original GolP-CHARMM force field ("GolP orig") is compared with our modified version including Lennard-Jones (LJ), harmonic (V_H) and Morse potential (V_M) interactions between S and Au(111).

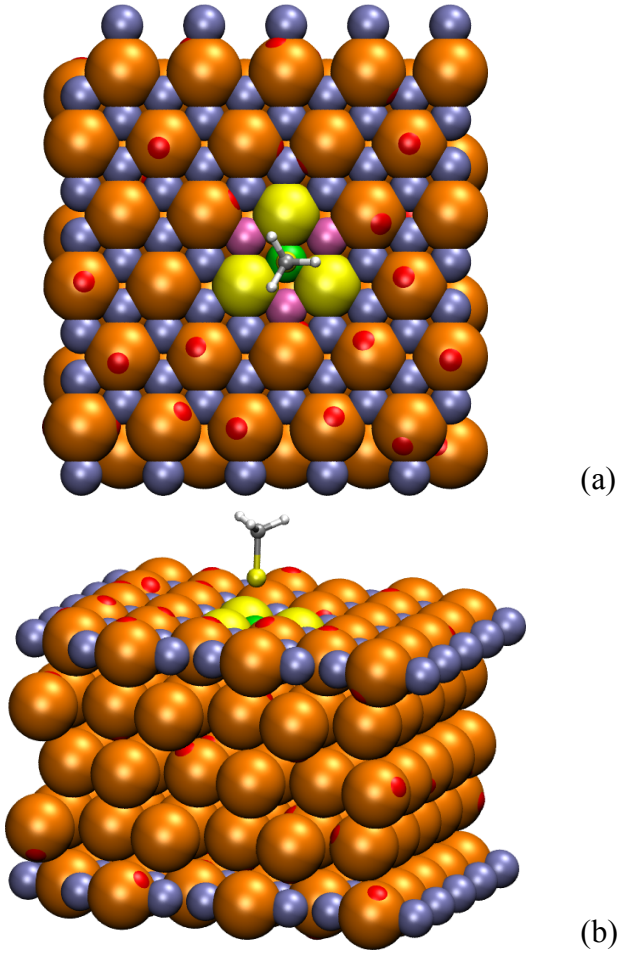

Figure 8: GolP-CHARMM atom types in the Au(111) slab with adsorption site: (a) top view, (b) side view. Particle colouring: orange = gold atoms with charged nucleus, red = dipole charge, yellow = neutral gold atom without dipole, blue = surface sites, purple = surface sites with smaller LJ radius, green = dummy site for molecular bonding.

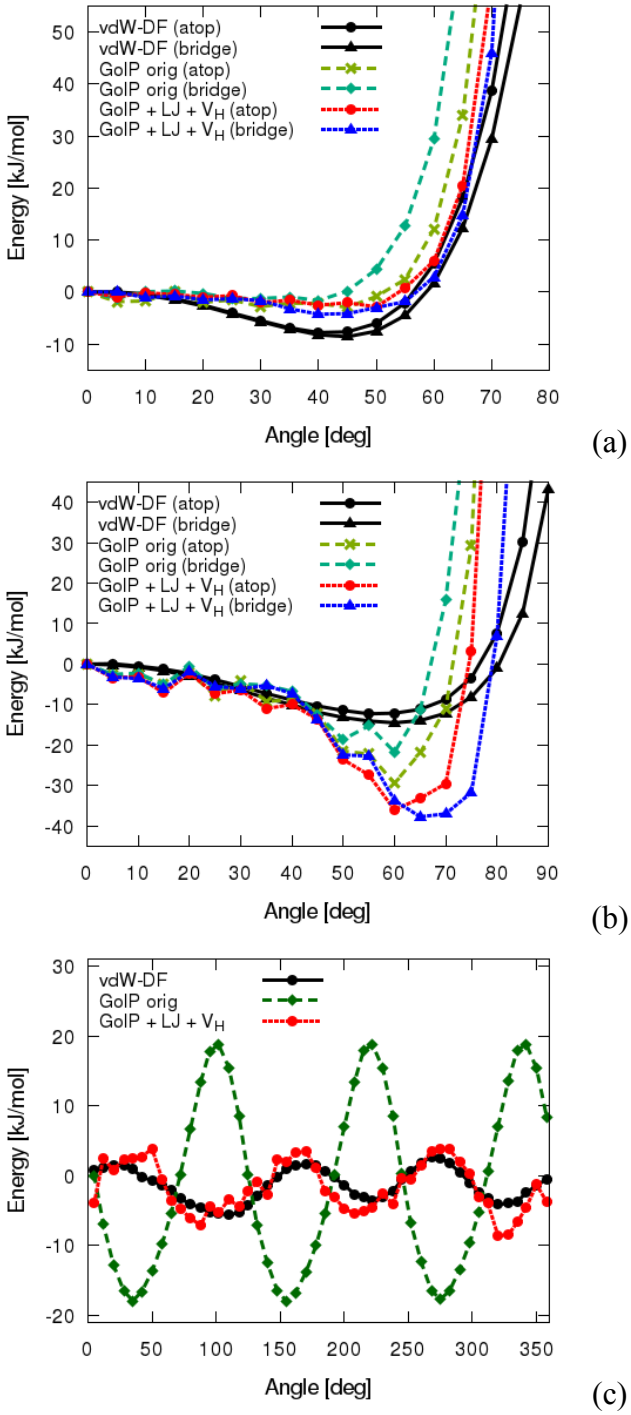

Figure 9: Angular potential-energy dependence of cysteine adsorbed on the fcc site of Au(111). The tilt angle to the surface normal is scanned for (a) methanethiolate (H_3C-S-) and (b) thiocyanate (NC-S-) while the rotation around the surface normal is shown for (c) cysteine thiolate (H_2N-CH(COOH)-S-).

TOC Graphic

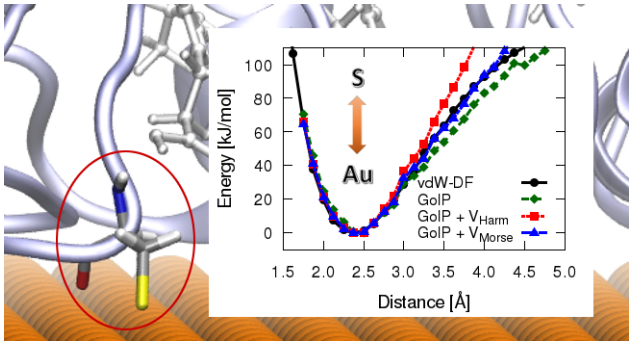
S
Au
Energy [kJ/mol]
100
80
60
40
20
0
1.5
2.0
2.5
3.0
3.5
4.0
4.5
5.0
Distance [Å]
vdW-DF
GoIP
GoIP + V_Harm
GoIP + V_Morse